Inorg. Chem. **2007**, *46*, 9201–9212

Synthesis, Photophysical, and Anion-Sensing Properties of Quinoxalinebis(sulfonamide) Functionalized Receptors and Their Metal Complexes

Tzu-Pin Lin, Chan-Yu Chen, Yuh-Sheng Wen, and Shih-Sheng Sun*

Institute of Chemistry, Academia Sinica, Nankang, Taipei 115, Taiwan, Republic of China

Received July 2, 2007

We report the synthesis, characterization, and photophysical properties of a series of organic receptors and their corresponding Re^{I} and Ru^{II} metal complexes as anion probes featuring bis(sulfonamide) interacting sites incorporating highly chromophoric π-conjugated quinoxaline moieties. The interactions with various anions were extensively investigated. These probe molecules are capable of recognizing F^-, OAc^-, CN^-, and $H_2PO_4^-$ with different sensitivities. The probe–anion interactions can be easily visualized via naked-eye colorimetric or luminescent responses. Probe **1** has the weakest acidic sulfonamide N–H protons and therefore simply forms hydrogen-bonding complexes with F^-, OAc^-, CN^-, and $H_2PO_4^-$. Probe **2** undergoes a stepwise process with the addition of F^- and OAc^-: formation of a hydrogen-bound complex followed by sulfonamide N–H deprotonation. Direct sulfonamide N–H deprotonation occurs upon the addition of CN^-, while only a hydrogen-bound complex forms with the $H_2PO_4^-$ ion for probe **2** in a dimethyl sulfoxide (DMSO) solution. Similar probe–anion interactions occur in probe **3** with the addition of F^-, CN^-, or $H_2PO_4^-$. However, only a genuine hydrogen-bound complex forms in the presence of the OAc^- ion in a DMSO solution of probe **3** because of the subtle difference in the pK_a values of sulfonamide N–H protons when probes **2** and **3** are compared. Coordination of probe **1** to a Re^{I} center or probe **2** to a Ru^{II} center increases the intrinsic acidity of sulfonamide N–H protons and results in an enhanced sensitivity to anions.

Introduction

The design and synthesis of artificial sensing systems capable of effectively detecting the presence of anions has received great current attention,[1] mostly because of the important roles that these anions play in biological and environmental issues.[2] In the design of anion receptors, various noncovalent interactions, such as electrostatic, hydrogen-bonding, coordination to a metal center, hydrophobicity, and a combination of any two or more of these, are utilized.

Among the various designs of synthetic receptors, the incorporation of luminescent chromophores, which are sensitive to interactions between the host and guest molecules, into the receptor has recently gained considerable attention because of their high sensitivity and low detection limit. The appeal of sensing systems containing luminescent chromophores stems from the high sensitivity of luminescence detection compared to other spectroscopic methods. The molecular sensing systems are designed to combine the ability to recognize and respond to an external input with mediation of an internal charge transfer,[3] photoinduced electron transfer,[4] excimer/exciplex emission,[5] exciton-migration-induced signal amplification in polymer luminescence,[6] or excited-state intramolecular proton transfer[7] as a

* To whom correspondence should be addressed. E-mail: sssun@chem.sinica.edu.tw.

(1) (a) Martínez-Máñez, R.; Sancenón, F. *Chem. Rev.* **2003**, *103*, 4419−4476 and references cited therein. (b) Beer, P. D.; Gale, P. A. *Angew. Chem., Int. Ed.* **2001**, *40*, 486−516.

(2) Schraderr, T., Hamilton, A. D., Eds. *Functional Synthetic Receptors*; Wiley-VCH: Weinheim, Germany, 2005.

(3) (a) Chen, C.-L.; Lin, T.-P.; Chen, Y.-S. Sun, S.-S. *Eur. J. Org. Chem.* **2007**, in press. (b) Chen, C.-L.; Chen, Y.-S.; Chen, C.-Y.; Sun, S.-S. *Org. Lett.* **2006**, *8*, 5053−5056. (c) Wu, F. Y.; Li, Z.; Guo, L.; Wang, X.; Lin, M. H.; Zhao, Y. F.; Jiang, Y. B. *Org. Biomol. Chem.* **2006**, *4*, 624−630. (d) Esteban-Gómez, D.; Fabbrizzi, L.; Licchelli, M. *J. Org. Chem.* **2005**, *70*, 5717−5720.

(4) (a) Tan, W.; Zhang, D.; Wang, Z.; Liu, C.; Zhu, D. *J. Mater. Chem.* **2007**, *17*, 1964−1968. (b) Lee, S. H.; Kim, S. H.; Kim, S. K.; Jung, J. H.; Kim, J. S. *J. Org. Chem.* **2005**, *70*, 9288−9295. (c) Thiagarajan, V.; Ramamurthy, P.; Thirumalai, D.; Ramakrishnan, V. T. *Org. Lett.* **2005**, *7*, 657−660.

(5) (a) Kim, H. J.; Kim, S. K.; Lee, J. Y.; Kim, J. S. *J. Org. Chem.* **2006**, *71*, 6611−6614. (b) Lee, J. Y.; Kim, S. K.; Jung, J. H.; Kim, J. S. *J. Org. Chem.* **2005**, *70*, 1463−1466. (c) Wu, J. S.; Zhou, J. H.; Wang, P. F.; Zhang, X. H.; Wu, S. K. *Org. Lett.* **2005**, *7*, 2133−2136. (d) Liao, J.-H.; Chen, C.-T.; Fang, J.-M. *Org. Lett.* **2002**, *4*, 561−564.

10.1021/ic701300a CCC: $37.00
Published on Web 09/15/2007

mode of signaling mechanism. The binding (interaction) of anionic species to the recognition sites leads to changes in certain properties of the receptors (such as color, luminescence, excited-state lifetime, etc.) that then serve as indicators of anion−receptor interactions.

The photophysical and photochemical properties of rhenium(I) and ruthenium(II) polypyridyl complexes have been extensively studied in the last 2 decades.[8] There are several examples showing that with the judicious design of the coordinating ligands these rhenium(I) and ruthenium(II) polypyridyl complexes can function as chemosensors of various analytes such as cations,[9] anions,[10] or biological molecules.[11] In particular, incorporating a positively charged Re^{I} or Ru^{II} center into the framework of sensory systems offers several advantages over pure organic sensory systems, leading to either the enhancement of the electrostatic interactions with negatively charged species or a higher probability of orbital overlap and, thus, stronger bonding interactions with anionic species. Moreover, rhenium(I) and ruthenium(II) polypyridyl complexes typically possess visible spectroscopic features with strongly allowed metal-to-ligand charge-transfer (MLCT) transition, which is to serve as a colorimetric indicator with high sensitivity to microenvironmental perturbation.[12]

For the receptors based on hydrogen bonds, the polarized N−H functional groups such as amide, urea (or thiourea), and pyrrole represent the most commonly seen anion interacting moiety in the literature.[13] In general, hydrogen-bond-induced π-electron delocalization or basic anion-induced N−H deprotonation serves as the signaling output of the anion−receptor interaction. Among the various polarized N−H functional groups, sulfonamide represents a less explored class for anion sensing.[7a,14] Previously, Crabtree and co-workers reported a neutral diphenylbenzene-1,2-disulfonamide receptor that shows high sensitivity and good selectivity to F^- over other halides.[14e] However, the lack of a chromophoric moiety in the molecule renders ^{1}H NMR spectroscopy the primary tool for monitoring the anion binding events. Starnes and co-workers later reported a porphyrin receptor fused with a quinoxalinebis(sulfonamide) moiety to show great selectivity for F^-.[14c] Moreover, the binding event could be traced by the shifting of a highly chromophoric Soret band in the porphyrin molecule. However, the general tedious and low-yield synthesis of porphyrin molecules of this kind has hindered its general usage in the area of chemical sensing. In a very recent report, Peng and co-workers have elegantly employed the sulfonamide group into a fluorescence sensing molecule that displays good optical differentiation of F^- and OAc^- based on the unique excited-state intramolecular proton-transfer property.[7a]

The anion-sensitive bis(sulfonamide) functionality could be easily modified to incorporate coordinating dipyridyl or phenanthroline moieties. We envision that introducing a transition-metal element into the framework of a sensing molecule via coordination of a dipyridyl or phenanthroline moiety would greatly enhance the detecting limit and the degree of interaction between the anion and the sensing molecule could be easily monitored with the optical color change accompanying the shift of the environmentally sensitive MLCT transition. Herein we report the synthesis and photophysical properties of a series of quinoxalinebis-(sulfonamide)-functionalized receptors and their corresponding Re^{I} or Ru^{II} metal complexes. The study of the anion binding properties of these anion probes allows us to correlate the anion−probe interaction mode and the electronic perturbation induced by anions.

Results and Discussion

Synthesis. Scheme 1 outlines the synthesis of sulfonamide-functionalized receptors and their corresponding transition-metal complexes. The organic probes **1**−**3** were synthesized by condensation of sulfonamide-functionalized diaminoben-

(6) (a) Wu, C.-Y.; Chen, M.-S.; Lin, C.-A.; Lin, S.-C.; Sun, S.-S. *Chem.*−*Eur. J.* **2006**, *12*, 2263−2269. (b) Zhou, G.; Cheng, Y.; Wang, L.; Jing, X.; Wang, F. *Macromolecules* **2005**, *38*, 2148. (c) Kim, T.-H.; Swager, T. M. *Angew. Chem., Int. Ed.* **2003**, *42*, 4803−4806. (d) Tong, H.; Wang, L.; Jing, X.; Wang, F. *Macromolecules* **2003**, *36*, 2584−2586.

(7) (a) Wu, Y.; Peng, X.; Fan, J.; Gao, S.; Tian, M.; Zhao, J.; Sun, S. *J. Org. Chem.* **2007**, *72*, 62−70. (b) Lee, J. K.; Na, J.; Kim, T. H.; Kim, Y. S.; Park, W. H.; Kim, J.; Lee, T. S. *Mater. Sci. Eng., C* **2004**, *24*, 261−264.

(8) (a) Vos, J. G.; Kelly, J. M. *Dalton. Trans.* **2006**, 4869−4883. (b) Sun, S.-S.; Lees, A. J. *Coord. Chem. Rev.* **2003**, *230*, 171−192. (c) Balzani, V.; Juris, A.; Venturi, M.; Campagna, S.; Serroni, S. *Chem. Rev.* **1996**, *96*, 759−833.

(9) (a) Li, M.-J.; Chu, B. W.-K.; Zhu, N.; Yam, V. W.-W. *Inorg. Chem.* **2007**, *46*, 720−733. (b) Lazarides, T.; Miller, T. A.; Jeffery, J. C.; Ronson, T. K.; Adams, H.; Ward, M. D. *Dalton Trans.* **2005**, 528−536. (c) Redman, J. E.; Beer, P. d.; Dent, S. W.; Drew, M. G. B. *Chem. Commun.* **1998**, 231−232. (d) MacQueen, D. B.; Schanze, K. S. *J. Am. Chem. Soc.* **1991**, *113*, 6108−6110.

(10) (a) Tzeng, B.-C.; Chen, Y.-F.; Wu, C.-C.; Hu, C.-C.; Chang, Y.-T.; Chen, C.-K. *New J. Chem.* **2007**, *31*, 202−209. (b) Lin, Z.-H.; Ou, S.-J.; Duan, C.-Y.; Zhang, B.-G.; Bai, Z.-P. *Chem. Commun.* **2006**, 624−626. (c) Sun, S.-S.; Lees, A. J.; Zavalij, P. Y. *Inorg. Chem.* **2003**, *42*, 3445−3453. (d) Mizuno, T.; Wei, W.-H.; Eller, L. R.; Sessler, J. L. *J. Am. Chem. Soc.* **2002**, *124*, 1134−1135. (e) Anzenbacher, P., Jr.; Tyson, D. S.; Jursíková, K.; Castellano, F. N. *J. Am. Chem. Soc.* **2002**, *124*, 6232−6233. (f) Uppadine, L. H.; Drew, M. G. B.; Beer, P. D. *Chem. Commun.* **2001**, 291−292. (g) Slone, R.; Yoon, D. I.; Calhoun, R. M.; Hupp, J. T. *J. Am. Chem. Soc.* **1995**, *117*, 11813−11814.

(11) (a) Lo, K. K.-W.; Sze, K.-S.; Tsang, K. H.-K.; Zhu, N. *Organometallics* **2007**, *26*, 3440−3447. (b) Cary, D. R.; Zaitseva, N. P.; Gray, K.; O'Day, K. E.; Darrow, C. B.; Lane, S. M.; Peyser, T. A.; Satcher, J. H., Jr.; Van Antwerp, W. P.; Nelson, A. J.; Reynolds, J. G. *Inorg. Chem.* **2002**, *41*, 1662−1669. (c) Deetz, M. J.; Smith, B. D. *Tetrahedron Lett.* **1998**, *39*, 6841−6844.

(12) (a) Huynh, M. H. V.; Dattelbaum, D. M.; Meyer, T. J. *Coord. Chem. Rev.* **2005**, *249*, 457−483. (b) Lees, A. J. *Coord. Chem. Rev.* **1998**, *177*, 3−35. (c) Chen, P.; Meyer, T. J. *Chem. Rev.* **1998**, *98*, 1439−1477.

(13) (a) Gale, P. A. Amide and urea based anion receptors. *Encyclopedia of Supramolecular Chemistry*; Marcel Dekker: New York, 2004; pp 31−41. (b) Gale, P. A.; Sessler, J. L.; Camiolo, S. Pyrrole- and polypyrrole-based anion receptors. *Encyclopedia of Supramolecular Chemistry*; Marcel Dekker: New York, 2004; pp 1176−1185. (c) Black, C. B.; Andrioletti, B.; Try, A. C.; Ruiperez, C.; Sessler, J. L. *J. Am. Chem. Soc.* **1999**, *121*, 10438−10439. (d) Gunnlaugsson, T.; Kruger, P. E.; Jensen, P.; Tierney, J.; Ali, H. D. P.; Hussey, G. M. *J. Org. Chem.* **2005**, *70*, 10875−10878. (e) Liu, B.; Tian, H. *J. Mater. Chem.* **2005**, *15*, 2681−2686. (f) Liu, B.; Tian, H. *Chem. Lett.* **2005**, *34*, 686−687.

(14) (a) Kavallieratos, K.; Sabucedo, A. J.; Pau, A. T.; Rodriguez, J. M. *J. Am. Soc. Mass Spectrom.* **2005**, *16*, 1377−1383. (b) Chen, C.-F.; Chen, Q.-Y. *Tetrahedron Lett.* **2004**, *45*, 3957−3960. (c) Starnes, S. D.; Arungundram, S.; Saunders, C. H. *Tetrahedron Lett.* **2002**, *43*, 7785−7788. (d) Kondo, S.-I.; Suzuki, T.; Yano, Y. *Tetrahedron Lett.* **2002**, *43*, 7059−7061. (e) Kavallieratos, K.; Bertao, C. M.; Crabtree, R. H. *J. Org. Chem.* **1999**, *64*, 1675−1683.

Scheme 1

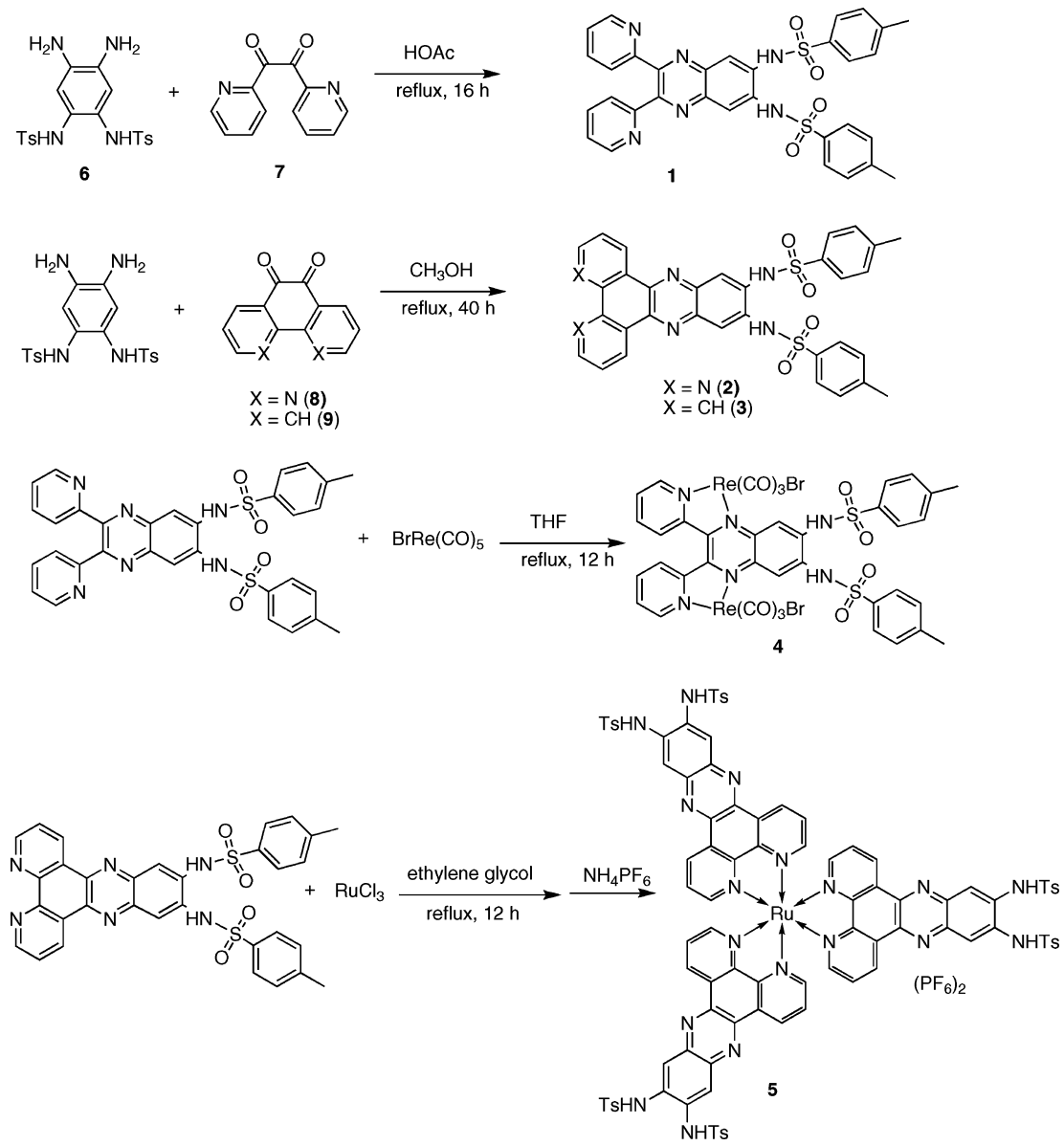

zene **6** and corresponding diketones **7**, **8**, or **9** in refluxing acetic acid or MeOH in high yield. The Re^{I} complex **4** was prepared by refluxing probe **1** and $BrRe(CO)_5$ in tetrahydrofuran (THF) with an essentially quantitative yield. The Ru^{II} complex **5** was obtained by heating a mixture of $RuCl_3$ and probe **2** in ethylene glycol at 150 °C followed by metathesis with KPF_6. Repeated recrystallization from hot acetonitrile afforded complex **5** in 14% yield. All new compounds have been fully characterized by ^1H NMR, mass spectrometry, and elemental analysis. The crystal structures of **1**, **3**, and **4** are further revealed by X-ray crystallography.

Crystal Structures. The structures of probes **1**, **3**, and **4** are illustrated in Figures 1−3, respectively. Crystallographic data are summarized in Table 1. Single crystals of probe **1** were obtained by layering a concentrated THF solution of **1** with diethyl ether. The ORTEP drawing of crystal **1** is depicted in Figure 1. Probe **1** crystallizes in the *monoclinic* space group $P2(1)/c$ with a pair of **1** cocrystallized in one unit cell. The two molecules of **1** arrange in an antiparallel fashion to form a dimer through a self-complementary double intermolecular hydrogen bond, with a pyridine nitrogen atom forming a hydrogen bond with a sulfonamide hydrogen atom of a symmetry-related molecule **1**. The other sulfonamide hydrogen atom forms an intramolecular hydrogen bond with an adjacent sulfonamide oxygen atom. Thus, the two sulfonamide N−H protons adopt a twisted syn−anti conformation. Two pyridine moieties are twisted out of the quinoxaline plane with dihedral angles of 60.7° and 32.6°.

Single crystals of probe **3** were grown from a saturated THF solution of **3** at 4 °C over several days. Probe **3** crystallizes in the triclinic space group $P\bar{1}$ with a pair of **3** cocrystallized in one unit cell. The ORTEP structure and packing diagram of **3** are shown in Figure 2. The two tosylate groups are twisted away from the phenanthrene−quinoxaline unit. An intramolecular hydrogen bonding exists between the sulfonyl oxygen atom and the other sulfonamide hydrogen atom. The extended rigid π-conjugated framework of the phenanthrene−quinoxaline unit in probe **3** displays a

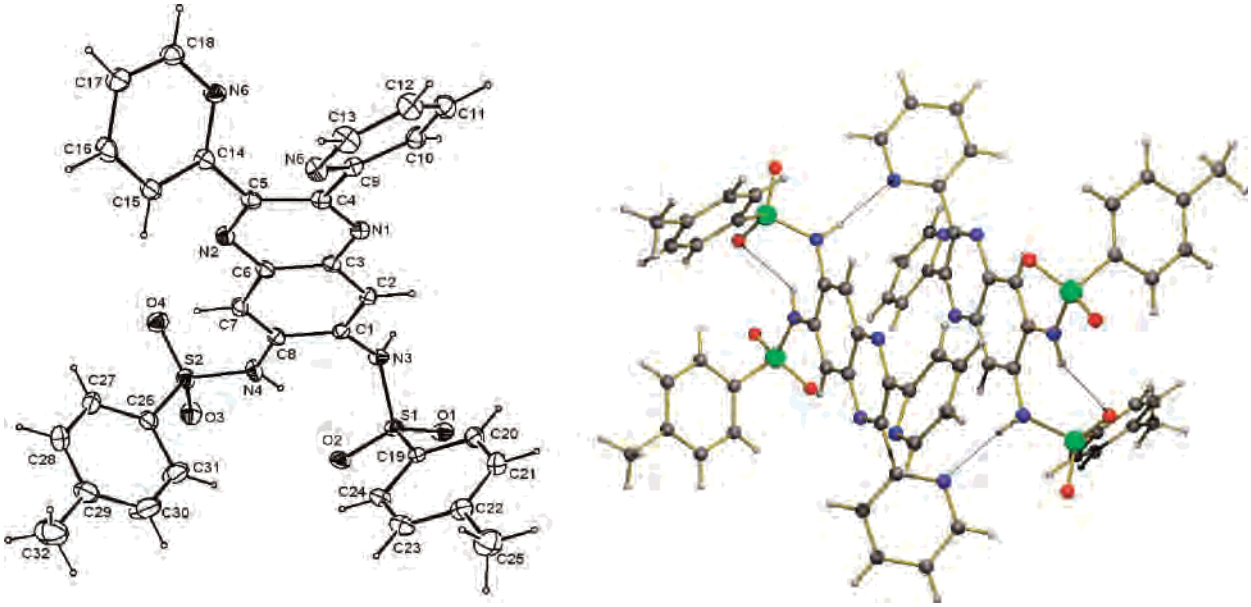

Figure 1. ORTEP representation of the crystal structure of probe **1** with 50% thermal probability ellipsoids (left) and a pair of probes **1** showing the hydrogen-bonding interactions (right).

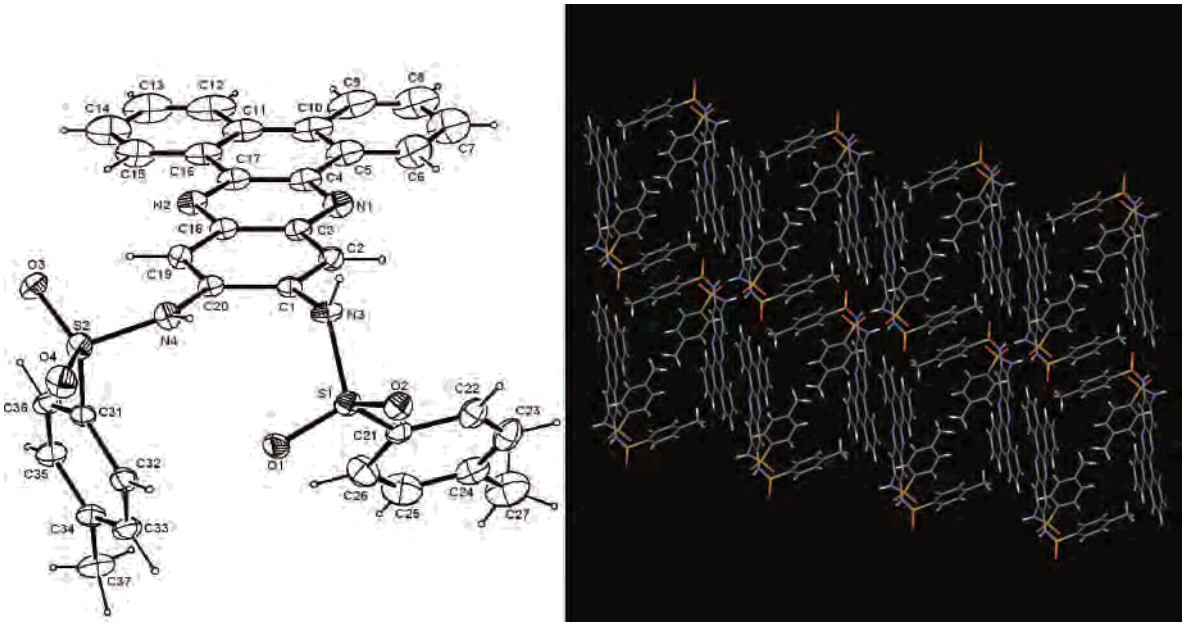

Figure 2. ORTEP representation of the crystal structure of probe **3** with 50% thermal probability ellipsoids (left) and packing diagram along the *b* axis (right).

noticeable π-stacking interaction within the crystal structure. Each phenanthrene−quinoxaline unit in probe **3** forms a π-stacking interaction with the adjacent phenanthroline−quinoxaline unit in the neighboring unit cell. The average distance is 3.42 Å.

Single crystals of probe **4** were grown by slow evaporation of a concentrated THF solution of **4**. The ORTEP diagram of **4** is shown in Figure 3. Probe **4** crystallizes in the *triclinic* space group $P\bar{1}$ with two cocrystallized THF solvents. Each crystal contains pairs of both conformational enantiomers in the unit cell. One THF molecule is disordered, while the other THF molecule forms a hydrogen bond with one sulfonamide N−H proton. The coordination geometries around the Re^{I} atoms are slightly distorted from the octahedral environment with a *facial* disposition for the three carbonyl groups. The carbonyl Re−C bond distances range from 1.874 to 1.946 Å. The Re−N bond distances range from 2.154 to 2.223 Å. The Re−C−O linkage [175.5(10)−178.7(7)°] does not deviate significantly from linearity. All determined carbonyl Re−C and Re−N bond distances appear to be normal.[10c,15]

Photophysical Properties. The absorption and emission spectral data along with lifetimes and emission quantum

(15) (a) Villegas, J. M.; Stoyanov, S. R.; Huang, W.; Rillema, D. P. *Dalton Trans.* **2005**, 1042−1051. (b) Lo, K. K.-W.; Lau, J. S.-Y.; Fong, V. W.-Y. *Organometallics* **2004**, *23*, 1098−1106. (c) Sun, S.-S.; Tran, D. T.; Zavalij, P. Y.; Oliver, S. R. J.; Lees, A. J. *Acta Crystallogr.* **2003**, *E59*, m134−136. (d) Sun, S.-S.; Anspach, J. A.; Lees, A. J. *Organometallics* **2002**, *21*, 685−693. (e) Yam, V. W. W.; Lo, K. K. W.; Cheung, K. K.; Kong, R. Y. C. *J. Chem. Soc., Chem. Commun.* **1995**, 1191−1193.

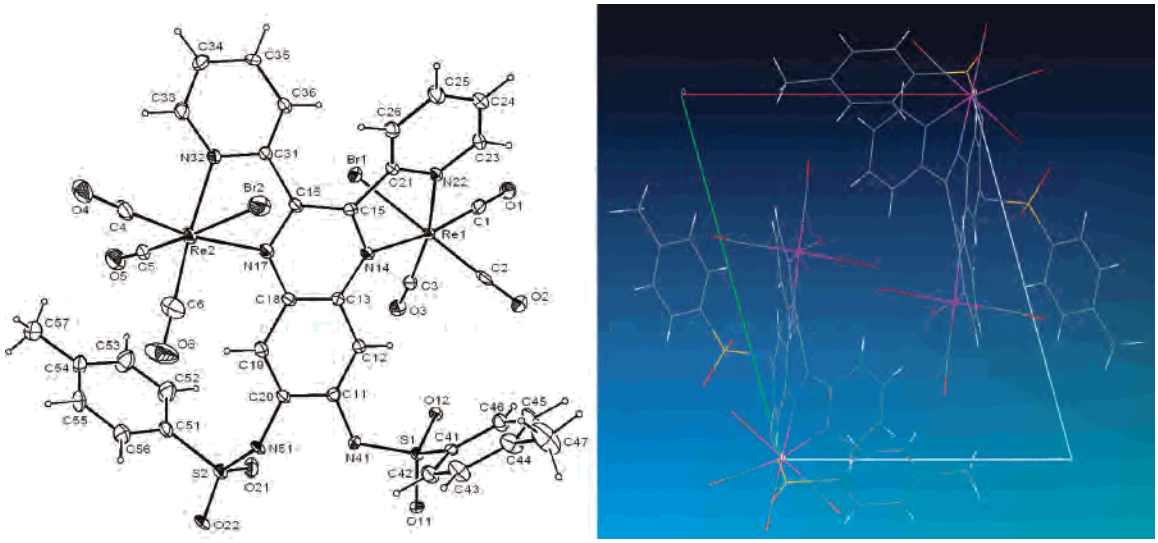

Figure 3. ORTEP representation of the crystal structure of probe **4** with 50% thermal probability ellipsoids (left) and a pair of probes **4** in one unit cell (right).

Table 1. Crystallographic Data for Probes **1**, **3**, and **4**

	1·**1**	**3**	**4**·2THF
empirical formula	$C_{64}H_{52}N_{12}O_8S_4$	$C_{34}H_{26}N_4O_4S_2$	$C_{46}H_{42}Br_2N_6O_{12}Re_2S_2$
M (g mol^{-1})	1245.42	618.71	1461.15
cryst syst	monoclinic	triclinic	triclinic
space group	$P2(1)/c$	$P\bar{1}$	$P\bar{1}$
a (Å)	15.4900(6)	10.4310(2)	9.6292(4)
b (Å)	24.4301(10)	11.9439(3)	12.7526(5)
c (Å)	19.9270(8)	14.7268(3)	21.3799(8)
α (deg)	90	100.2090(10)	79.0800(10)
β (deg)	93.187(2)	98.8850(10)	89.9460(10)
γ (deg)	90	108.0950(10)	75.0180(10)
V (Å^3)	7529.2(5)	1672.82(6)	2487.03(17)
Z	4	2	2
R1 (all, $>2\sigma$)	0.0929, 0.0510	0.0629, 0.0409	0.0498, 0.0356
wR2 (all, $>2\sigma$)	0.1321, 0.1236	0.0988, 0.0957	0.1061, 0.0997

Table 2. Photophysical Properties of Probes **1**−**5** in a CH_3CN[a] or DMSO[b] Solution at 293 K

	absorption	emission				
probe	λ_{max}, nm ($10^{-3}\epsilon$, M^{-1} cm^{-1})	λ_{em}, nm	Φ_{em}	τ, ns	k_r, s^{-1}	k_{nr}, s^{-1}
1	261 (37.5), 355 (13.2), 415 (0.6)	530	0.05	1.2	4.2×10^7	7.9×10^8
2	276 (56.3), 332 (28.9), 462 (16.8)	590	0.67	10.4	6.4×10^7	3.2×10^7
3	282 (56.7), 320 (28.2), 460 (16.3)	574	0.59	9.1	6.5×10^7	4.5×10^7
4	324 (19.3), 439 (11.4), 550 (5.7, sh)	608	2.6×10^{-5}	<0.1[c]		
5	271 (109), 337 (84.5), 493 (79.9)	604	5.6×10^{-4}	8.9	6.3×10^4	1.1×10^8

[a] For probes **1** and **4**. [b] For probes **2**, **3**, and **5**. [c] The excited-state lifetime is too short to be precisely measured in our instrument.

yields of probes **1**−**5** are summarized in Table 2. Probes **1**−**3** display a series of absorption bands in the UV−visible region, where the absorptions can be assigned to $\pi-\pi^*$ transitions. In contrast to the white to pale yellow color of ligands **1**−**3**, both complexes **4** and **5** are reddish-brown in the solid state. For complex **4** in CH_3CN, the absorption bands at 324 and 439 nm are assigned to ligand-centered $\pi-\pi^*$ transitions. The less intense absorption shoulder appearing at ca. 550 nm is assigned to a spin-allowed metal ($Re_{d\pi}$)-to-ligand (π^*) charge-transfer (^{1}MLCT) transition.[16] Similarly, complex **5** in dimethyl sulfoxide (DMSO) exhibits two absorptions in the UV region that are assigned to ligand-centered $\pi-\pi^*$ transitions, and the absorption band at 493 nm is assigned to a spin-allowed metal ($Ru_{d\pi}$)-to-ligand (π^*) charge-transfer (^{1}MLCT) transition.[8c,17] We envision that the incorporation of a MLCT character in the probe molecules that is particularly sensitive to the surrounding microenvironment,[18] a property that is essential for molecular recogni-

(16) (a) Dinofo, P. H.; Coropceanu, V.; Brédas, J.-L.; Hupp, J. T. *J. Am. Chem. Soc.* **2006**, *128*, 12592−12593. (b) Walters, K. A.; Ley, K. D.; Cavalaheiro, C. S. P.; Miller, S. E.; Gosztola, D.; Wasielewski, M. R.; Bussandri, A. P.; van Willigen, H.; Schanze, K. S. *J. Am. Chem. Soc.* **2001**, *123*, 8329−8342. (c) Sun, S.-S.; Lees, A. J. *J. Am. Chem. Soc.* **2000**, *122*, 8956−8967. (d) Baba, A. I.; Shaw, J. R.; Simon, J. A.; Thymmel, R. P.; Schmehl, R. H. *Coord. Chem. Rev.* **1998**, *171*, 43−59. (e) Stoeffler, H. D.; Thornton, N. B.; Temkin, S. L.; Schanze, K. S. *J. Am. Chem. Soc.* **1995**, *117*, 7119−7128. (f) Baiano, J. A.; Kessler, R. J.; Lumpkin, R. S.; Munley, M. J.; Murphy, W. R., Jr. *J. Phys. Chem.* **1995**, *99*, 17680−17690. (g) Worl, L. A.; Duesing R.; Chen, P.; Ciana, L. D.; Meyer, T. J. *J. Chem. Soc., Dalton Trans.* **1991**, 849−858. (h) Caspar, A. J.; Meyer, T. J. *J. Phys. Chem.* **1983**, *87*, 952−957.

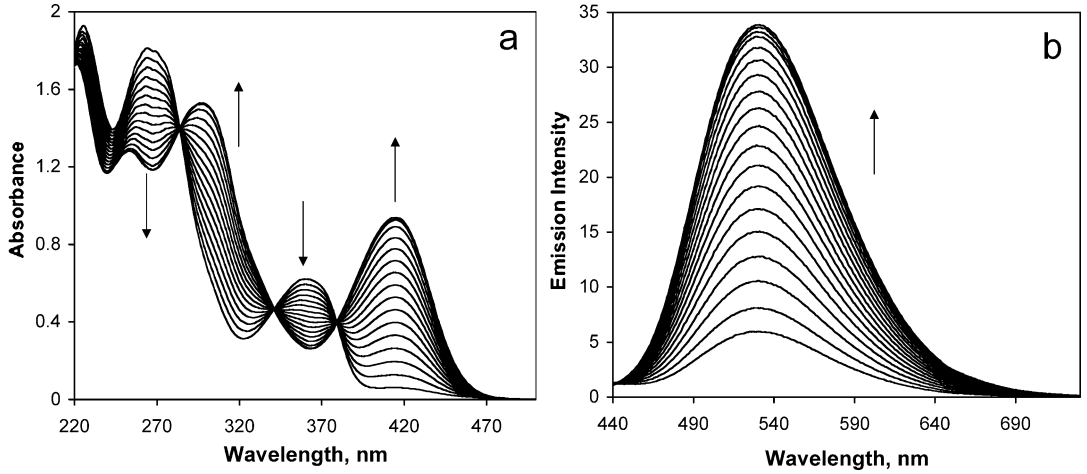

Figure 4. Absorption (a) and emission (b) spectral traces of probe **1** (4.6×10^{-5} M) in an acetonitrile solution upon the addition of *n*-Bu_4NF [$(0-4.6) \times 10^{-5}$ M].

tion, would effectively promote the optical detecting limit and provide a more sensitive way to distinguish the incoming anionic substrates.

Organic probes **2** and **3** show strong luminescence in an air-equilibrated solution with excited-state lifetimes of ca. 10 ns. On the other hand, probe **1** displays a much weaker emission and shorter lifetime compared to **2** and **3**. Giving roughly the same order of radiative rate constants among **1**−**3** but over an order higher of nonradiative rate constant in **1** when compared to **2** and **3** suggests that the more flexible structure of **1** may directly contribute to the greater nonradiative decay of the emissive state. The relatively high quantum yields and short lifetimes suggest that the emission for **1**−**3** originates from a singlet $\pi-\pi^*$ excited state.

Upon coordination to Re^I or Ru^{II}, the luminescence for both complexes **4** and **5** is only detectable in a deoxygenated solution with extremely low quantum yields while the emission is completely quenched in an air-equilibrated solution. The luminescence of rhenium(I) and ruthenium(II) polypyridyl complexes typically originates from the lowest ^{3}MLCT excited state because of the large spin orbital coupling exerted by Re^I and Ru^{II}, and their decay follows the energy gap law where the nonradiative decay process becomes more efficient when the energy gap between the ground state and the emissive excited state is smaller because of greater vibrational overlap with the two electronic states.[16,17] Therefore, luminescence decay for both complexes **5** and **6** is assigned to the ^{3}MLCT excited state and is anticipated to be dominated by a nonradiative process with the fully π-conjugated structural framework of the ligands **1** and **2** to effectively lower the ligand π^* level and the resulting small energy gap. The consequence is the observation of low luminescence quantum yields and short lifetimes for both complexes **4** and **5** even in a deoxygenated solution.

Anion Binding Studies by Absorption, Emission, and ^{1}H NMR Titrations. The anion binding properties of probes **1**−**5** have been investigated by absorption and luminescent titrations. In some cases, ^{1}H NMR titrations were also carried out to clarify the probe−anion interaction modes. Of the 10 anions we studied (F^-, Cl^-, Br^-, I^-, CN^-, OAc^-, $H_2PO_4^-$, HSO_4^-, NO_3^-, and ClO_4^-), all probes **1**−**5** show various degrees of response only to F^-, OAc^-, CN^-, and $H_2PO_4^-$. Probe **4** also shows a very weak colorimetric response to Cl^-. Figure 4 illustrates absorption and emission titrations of probe **1** upon the addition of F^- in a CH_3CN solution. In the electronic absorption spectrum, the tail at ~415 nm starts to grow accompanied with a decrease of the band at 355 nm and, concomitantly, the emission intensity at 530 nm shows an enhancement upon the addition of a F^- ion. The appearance of a set of clean isosbestic points indicates that the binding of F^- to probe **1** is a clean equilibrium process. With reference to the spectroscopic studies of related sulfonamide compounds,[7a,14c] it is likely that the change in the absorption and emission spectra is a consequence of the hydrogen bonding of F^- to the sulfonamide N−H protons. Similar trends of spectral changes have been observed in absorption and emission spectra for probe **1** upon the addition of OAc^-, CN^-, or $H_2PO_4^-$ in a CH_3CN solution.

The UV−visible absorption traces were further analyzed over the entire wavelength range using a nonlinear least-squares fit algorithm as implemented in the *SPECFIT* software package to extract the corresponding equilibrium constants. The obtained equilibrium constants are compiled in Table 3. In general, probe **1** exhibits high sensitivity to CN^-, OAc^-, and F^- but, nevertheless, lacks good selectivity to explicitly differentiate these three anions.

The addition of anions into a DMSO solution of probes **2** or **3** resulted in different spectroscopic titration profiles compared to the results from probe **1** in CH_3CN. In general, the spectrophotometric titration profiles of probes **2** and **3** with the addition of anions are essentially the same. Figure 5 shows the absorption spectral changes of probe **2** upon the addition of *n*-Bu_4NF in a DMSO solution. The absorption band at 462 nm slightly increased with the progressive

(17) (a) Schlicke, B.; Belser, P.; De Cola, L.; Sabbioni, E.; Balzani, V. *J. Am. Chem. Soc.* **1999**, *121*, 4204−4214. (b) Mecklenburg, S. L.; Peek, B. M.; Schoonover, J. R.; McCafferty, D. G.; Wall, C. G.; Erickson, B. W.; Meyer, T. J. *J. Am. Chem. Soc.* **1993**, *115*, 5479−5495. (c) Juris, A.; Balzani, V.; Barigelletti, F.; Campagna, S.; Belser, P.; von Zelewsky, A. *Coord. Chem. Rev.* **1988**, *84*, 85−277.
(18) Lees, A. J. *Comments Inorg. Chem.* **1995**, *17*, 319−346.

Table 3. Equilibrium Constants for Probes **1**−**5** in a CH_3CN[a] or DMSO[b] Solution at 20 °C Determined by Absorption Spectroscopic Titrations

	equilibrium constant K[c]				
anion	probe **1**	probe **2**	probe **3**	probe **4**	probe **5**
F^-	$K_a = 2.5 \times 10^4$	$K_a = 4.0 \times 10^5$ $K_d = 7.1 \times 10^3$	$K_a = 1.4 \times 10^5$ $K_d = 1.2 \times 10^2$	$K_a = 3.1 \times 10^6$ $K_d = 1.1 \times 10^4$	$K_a = 1.3 \times 10^6$ $K_d = 7.3 \times 10^4$
CN^-	$K_a = 2.3 \times 10^5$	$K_d = 7.9 \times 10^3$	$K_d = 5.9 \times 10^3$	$K_{d1} = 6.4 \times 10^6$ $K_{d2} = 1.2 \times 10^6$	$K_{d1} = 9.8 \times 10^5$ $K_{d2} = 6.8 \times 10^3$
OAc^-	$K_a = 1.3 \times 10^5$	$K_a = 1.7 \times 10^5$ $K_d = 2.4 \times 10^3$	$K_a = 6.7 \times 10^5$	$K_{d1} = 1.4 \times 10^6$ $K_{d2} = 1.8 \times 10^3$	$K_a = 1.8 \times 10^6$ $K_d = 1.9 \times 10^4$
$H_2PO_4^-$	$K_a = 2.3 \times 10^3$	$K_a = 1.9 \times 10^4$	$K_a = 8.8 \times 10^3$	$K_a = 2.8 \times 10^4$	$K_a = 2.9 \times 10^5$ $K_d = 1.1 \times 10^2$
Cl^-	$K_a = 1.2 \times 10^2$	$K_a = 2.1 \times 10^2$	$K_a = 1.7 \times 10^2$	$K_a = 6.5 \times 10^3$	$K_a = 1.3 \times 10^3$
OH^-		$K_d = 2.2 \times 10^3$	$K_d = 1.3 \times 10^3$	$K_{d1} = 5.5 \times 10^6$ $K_{d2} = 2.6 \times 10^6$	$K_{d1} = 7.0 \times 10^4$ $K_{d2} = 4.9 \times 10^3$

[a] For probes **1** and **4**. [b] For probes **2**, **3**, and **5**. [c] The anions were added as tetrabutylammonium salts. K_a and K_d represent the association constants of anion−probe hydrogen-bonding complexes and proton dissociation constants of probe molecules, respectively.

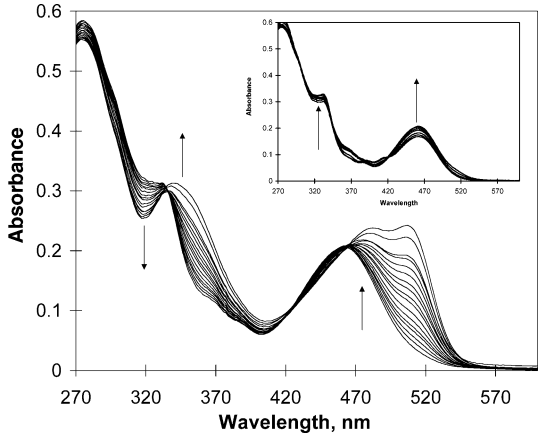

Figure 5. Absorption spectral titrations of probe **2** (1.1×10^{-5} M) in DMSO upon the addition of *n*-Bu_4NF (1.1×10^{-5}−4.5×10^{-4} M). The inset shows the addition of *n*-Bu_4NF up to 1 equiv [$(0-1.1) \times 10^{-5}$ M].

addition of F^- up to 1 equiv. After more than 1 equiv of F^- was added, however, a new tailing absorption band appeared at 506 nm and was intensified with new isosbestic points appearing at 463 and 333 nm. The stepwise absorption spectral change is ascribed to the formation of an initial hydrogen bonding between sulfonamide N−H protons and F^- followed by neat proton transfer to form a stable HF_2^- anion, which was further confirmed by ^{1}H NMR titration experiments (vide infra).[19]

The interactions of probes **2** and **3** with OAc^-, CN^-, and $H_2PO_4^-$ were also studied. Unlike the titration profiles of F^-, the addition of CN^- into a DMSO solution of probe **2** or **3** resulted in deprotonation of the sulfonamide N−H with an apparent one-step process with clear isosbestic points at 459, 423, and 333 nm. The Job plot confirms the 1:1 stoichiometry for cyanide−probe **2** and cyanide−probe **3** interactions. The very minor changes in absorption spectral traces of **2** and **3** upon the addition of $H_2PO_4^-$ implied only a hydrogen-bonding interaction, which is supported by the ^{1}H NMR titration experiment. where the aromatic protons shifted slightly upfield on the addition of up to 1 equiv of $H_2PO_4^-$ and no further shifting was observed with the addition of excess $H_2PO_4^-$ (Figures S1 and S2 in the Supporting Information). It should be noted here that the sulfonamide N−H signals were too broad to observe in the ^{1}H NMR spectra because of the rapid proton exchange in the presence of a trace amount of water in a deuterated DMSO solvent.

Figure 6 displays the ^{1}H NMR titration spectra for titration of a DMSO-d_6 solution probe **2** with F^- and CN^-. Upon the addition of CN^- (Figure 6a), all proton signals shifted progressively upfield, with the greatest shift observed for the singlet signal of quinoxaline protons ($\Delta\delta = -0.47$ ppm with the addition of 5 equiv of CN^-). The upfield shift of proton signals in conjunction with the significant bathochromic shift in the UV−visible spectra indicates an increasing shielding effect on the protons and suggests neat proton transfer occurring from the sulfonamide N−H to CN^-. The stoichiometry of the cyanide−probe **2** interaction is confirmed to be 1:1, which indicates that only one sulfonamide N−H proton was deprotonated by the CN^- ion.

On the other hand, the addition of F^- up to 1 equiv induced an upfield shift for all aromatic protons. The chemical shifts of all protons essentially remained the same between 1 and 2 equiv additions of F^- and did not move further to upfield positions until the added F^- concentration was over 2 equiv (Figure 6b). This observation along with the stepwise absorption spectral profiles shown in Figure 5 suggests that a hydrogen-bound complex formed first followed by neat proton transfer with the addition of over 2 equiv of F^- to generate deprotonated **2** and a highly stable HF_2^- anion.[20] It is known that two F^- ions together behave as a very strong base with $pK_a = 32$ in DMSO.[21] Similar spectral responses with the addition of CN^- and F^- were also observed with analogous ^{1}H NMR experiments carried out for probe **3** in a DMSO-d_6 solution (Figures S3 and S4 in the Supporting Information).

Upon the addition of OAc^- into a DMSO solution of probe **2**, very similar spectral traces to the cases of F^- were observed in both absorption and ^{1}H NMR titrations (Figure S5 in the Supporting Information) with apparent two-step processes. This observation is likewise due to the formation of hydrogen-bound complex **2**···OAC^- in the first stage with

(19) (a) Amendola, V.; Esteban-Gómez, D.; Fabbrizzi, L.; Licchelli, M. *Acc. Chem. Res.* **2006**, *39*, 343−353. (b) Boiocchi, M.; Del Boca, L.; Esteban-Gómez, D.; Fabbrizzi, L.; Licchelli, M.; Monzani, E. *J. Am. Chem. Soc.* **2004**, *126*, 16507−16514.

(20) Gronert, S. *J. Am. Chem. Soc.* **1993**, *115*, 10258−10266.

(21) Bordwell, F. G. *Acc. Chem. Res.* **1988**, *21*, 456−463.

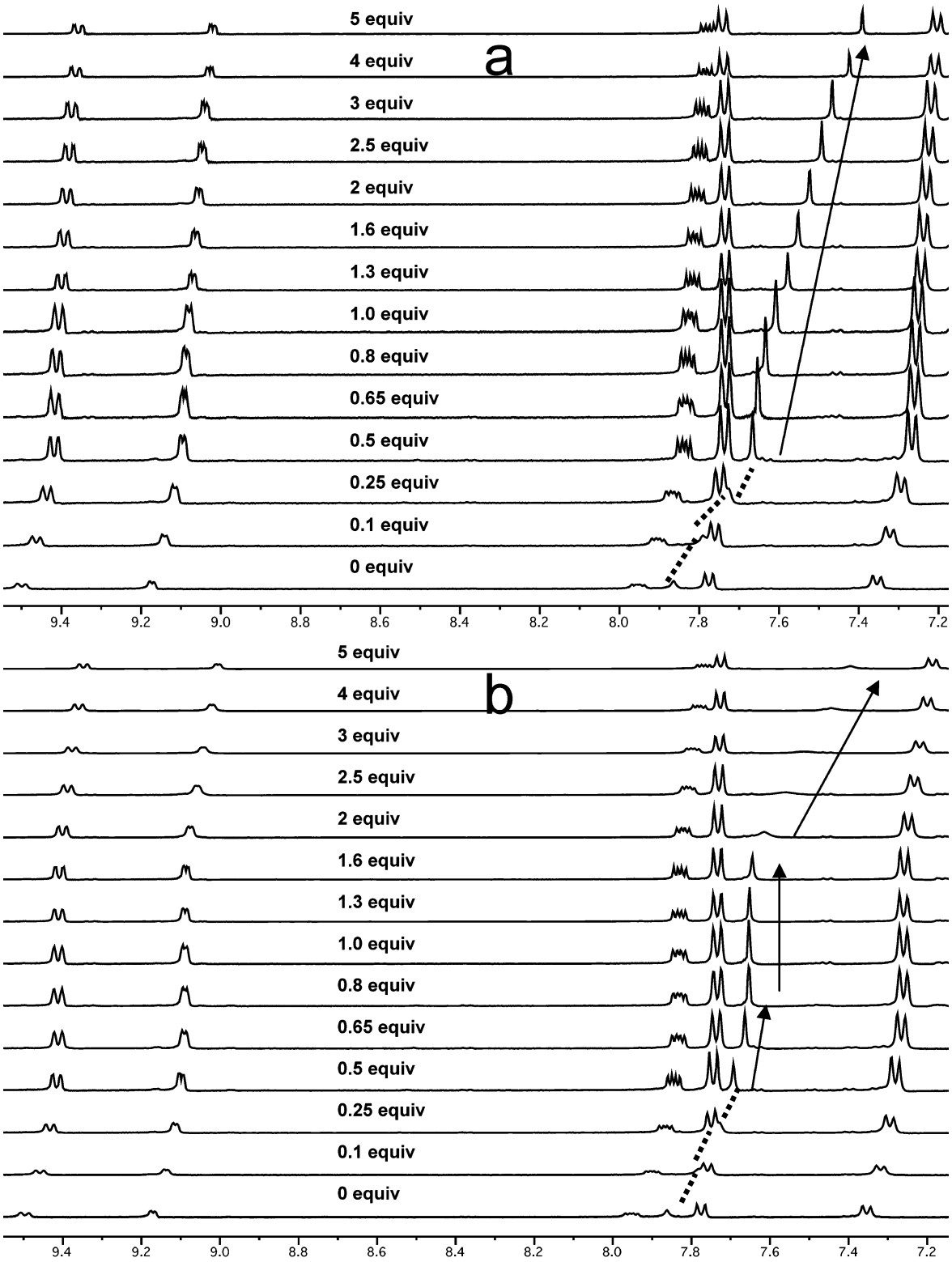

Figure 6. ^{1}H NMR spectra of probe **2** in DMSO-d_6 with the addition of *n*-Bu_4NCN (a) and *n*-Bu_4NF (b).

a low OAc^- concentration followed by neat proton transfer in the presence of a high OAc^- concentration to produce deprotonated **2** and a stable $(CH_3COOH\cdots OOCCH_3)^-$ anion dimer in solution.[7a,22] On the other hand, only a single set of isosbestic points appears in the absorption spectral traces for probe **3** with the addition of OAc^- in a DMSO solution. The quinoxaline proton signal shifts to an upfield position with up to a 1 equiv addition of OAc^- during the ^{1}H NMR titrations and virtually does not shift with a higher concentration of OAc^- (Figure S6 in the Supporting Information). This result along with the 1:1 stoichiometry determined by the Job plot suggests that probe **3** can only establish the

(22) Boiocchi, M.; Del Boca, L.; Esteban-Gómez, D.; Fabbrizzi, L.; Licchelli, M.; Monzani, E. *Chem.—Eur. J.* **2005**, *11*, 3097−3104.

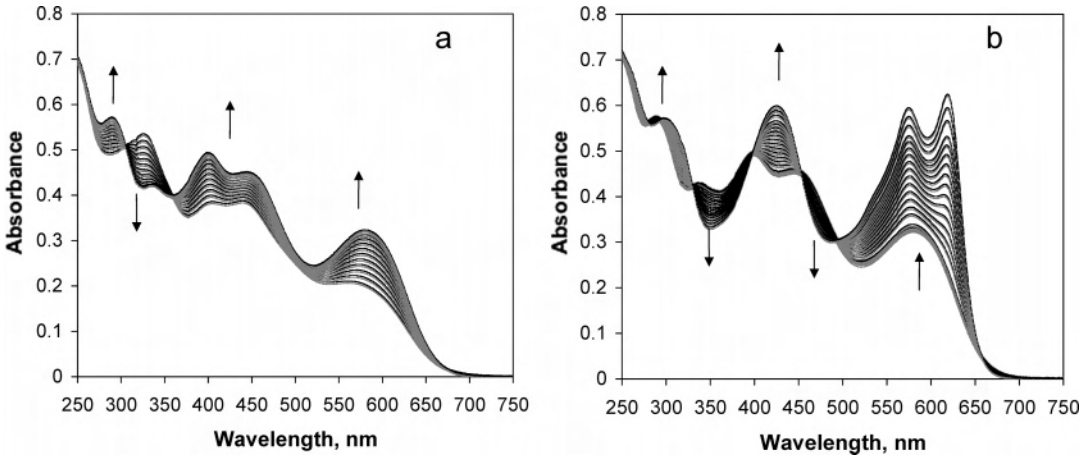

Figure 7. Electronic absorption spectral traces of probe **4** (2.5×10^{-5} M) in CH_3CN upon the addition of *n*-Bu_4NF: (a) $[F^-] = (0-2.8) \times 10^{-5}$ M; (b) $[F^-] = 2.8 \times 10^{-5}-1.1 \times 10^{-4}$ M.

hydrogen-bonding interaction with the incoming OAC^- ion, which is in accordance with the weaker acidity of the sulfonamide N−H protons in probe **3** than that of the sulfonamide N−H protons in probe **2**.

The equilibrium constants obtained from spectral fitting are also collected in Table 3. The most basic CN^- ion results in a single deprotonation for both probes **2** and **3** with similar dissociation constants. The association constants for the formation of hydrogen-bound complexes of probes **2** and **3** with F^- and OAC^- are comparable and about 1 order higher than that with $H_2PO_4^-$ in a highly polar DMSO solution. It is apparent that the capability of establishing a hydrogen-bonding interaction for probes **2** and **3** is in the same order. However, the subtle variation in the structures of probes **2** and **3** (phenanthroline−quinoxaline vs phenanthrene−quinoxaline) results in a totally different interacting mode toward the OAC^- ion: a stepwise hydrogen-bonding formation followed by neat proton transfer in probe **2** vs a genuine hydrogen-bonding interaction in probe **3**.

The pK_a values of sulfonamide N−H protons in probes **1** and **2** are expected to become smaller upon coordination of Lewis acidic metal centers on the pyridylquinoxaline moiety of **1** and the phenanthroline moiety of **2**. The overall effect is to effectively increase the sensitivity of the metal complex probes **4** and **5** to anions. In addition, the increasing acidity of the sulfonamide N−H protons also facilitates the tendency of neat proton transfer from probe molecules to basic anions.

Indeed, the addition of F^- to an acetonitrile solution of probe **4** resulted in an increase in the ^{1}MLCT absorption band with sharp isosbestic points at 305 and 354 nm (Figure 7a), indicating a clean well-defined equilibrium in solution. After more than 1 equiv of F^- was added, however, the ^{1}MLCT absorption band was further intensified and red-shifted, with a new set of isosbestic points appearing at 287, 330, 396, 452, and 492 nm (Figure 7b). Similar two-step equilibrium phenomena were also observed in the titration of CN^- or OAC^- to the solution of probe **4**. Job plots confirm the 1:2 stoichiometry between probe **4** and these anions. However, only one equilibrium was observed in the UV−visible absorption response similar to the profile shown in Figure 8a upon the addition of $H_2PO_4^-$ or Cl^- ions, and the Job plots show a 1:1 stoichiometry for both anions.

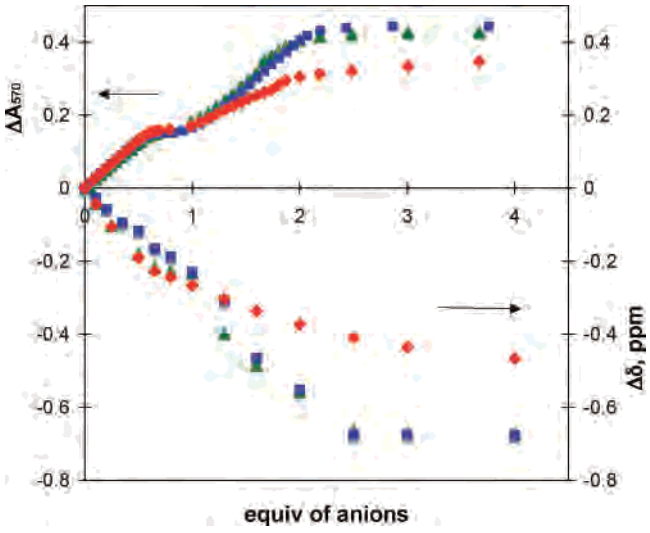

Figure 8. UV−visible absorption (left, *y* axis) and ^{1}H NMR (right, *y* axis) spectral profiles of probe **4** with the addition of CN^- (green triangle curve), OAC^- (red diamond curve), and OH^- (blue square curve).

The stepwise process observed in the spectrophotometric titration with F^- can be described by two stepwise equilibria: (1) formation of a hydrogen-bound complex via sulfonamide N−H protons with an incoming anion followed by (2) deprotonation of the acidic sulfonamide N−H proton to form mono-deprotonated probe **4** and HF_2^-. The ^{1}H NMR titration of probe **4** with the addition of *n*-Bu_4NF gives spectral traces similar to the cases of probes **2** and **3**. In other words, a hydrogen-bond-induced upfield shift was observed in the singlet signal of quinoxaline upon the addition of a first 1 equiv of F^- in a CD_3CN solution of probe **4**. The proton signals virtually do not move between additions of 1−2 equiv of F^-. Subsequently, further upfield shifts of the proton signals are observed again with the amount of added F^- over 2 equiv (see Figure S7 in the Supporting Information).

In the cases of CN^- and OAc^-, the spectrophotometric responses are attributed to a stepwise double deprotonation. Probe **4** was further titrated by *n*-Bu_4NOH to confirm that

the double deprotonation indeed occurred during the course of CN^- and OAc^- titration. The very similar titration isotherms of the absorption band at 570 nm as well as the upfield shift of the quinoxaline proton signals upon the addition of OH^-, CN^-, and OAc^- shown in Figure 8 (see Figures S8−S13 in the Supporting Information for UV−visible absorption and ^1H NMR spectral traces of individual titrations) strongly suggest that probe **4** undergoes a stepwise double proton transfer in the presence of CN^- or OAc^-. The less basic $H_2PO_4^-$ and Cl^- ions show no ability to deprotonate the sulfonamide N−H protons, where the proton signals upfield shift and reach the maximum shift at the 1 equiv addition of $H_2PO_4^-$ (see Figure S14 in the Supporting Information) and, thus, form only simple 1:1 hydrogen-bonding complexes with probe **4**.

The stretching frequencies of the metal carbonyl in probe **4** provide an additional channel to probe the remote probe−anion interactions.[23] The typical CO stretching frequencies of metal carbonyl complexes appear at 1700−2100 cm^{-1}, a region that is usually free of other ligand vibrations. With the Re^I site symmetry of C_s, the IR ν(CO) bands of probe **4** are typical of three CO stretches: two of A′ symmetry and one of A″ symmetry.[24] The extent of Re^I π back-bonding to the metal carbonyl would be directly correlated to the electron density on the chelating dipyridylquinoxanline ligand. In other words, one would expect that the higher electron density on the chelating ligand would result in a stronger π back-bonding to the Re^I−C bond and, thus, reduce the IR stretching frequencies of the metal carbonyl.

On the basis of the results obtained from ^1H NMR and UV−visible spectrophotometric titration experiments, the electron density of the chelating dipyridylquinoxanline ligand is expected to increase with the formation of a hydrogen bond and/or deprotonation of the sulfonamide N−H by the incoming anions. Indeed, the IR ν(CO) bands of probe **4** shift to lower frequencies upon anion addition. Figure 9 illustrates the shift of the IR ν(CO) bands of probe **4** upon the addition of F^- in a CH_3CN solution. The shift of the carbonyl group frequency is in the order of $CN^- > F^- \approx OAc^- > H_2PO_4^- > Cl^-$, which is consistent with the results obtained from ^1H NMR and UV−visible spectrophotometric titrations.

The addition of F^- to a DMSO solution of probe **5** induces spectral changes similar but more sensitive to the spectral responses of probe **2**, which is the ligand of probe **5**. The spectral traces can be separated to a two-step process (Figure 10). The absorption band at 493 nm is intensified upon the addition of F^- up to 1 equiv followed by a growth of a new band at 534 nm. This newly formed absorption band matches well with the absorption band formed in the titration spectra of *n*-Bu_4NOH (Figure S15 in the Supporting Information), and therefore it is assigned to originate from a deprotonated species. Thus, the spectral changes in the first process are

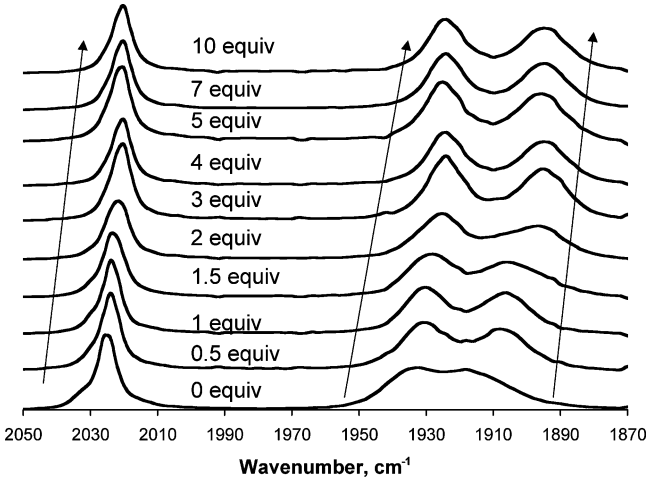

Figure 9. Changes of ν(CO) of probe **4** in the IR spectra upon the addition of *n*-Bu_4NF in a CH_3CN solution.

attributed to the formation of a hydrogen-bound complex followed by neat proton transfer in the second process. The stoichiometry of the fluoride−probe **5** interactions is confirmed to be 2:1 from the Job plot.

Similar spectral responses were also observed for OAc^- and $H_2PO_4^-$, albeit with less sensitivity. Accordingly, the two-step process for F^- can also be applied to OAc^- and $H_2PO_4^-$, which are also known to form relatively stable hydrogen-bound dimers.[22] The absorption spectral titration profile with the addition of CN^- also resembles the profile with the addition of OH^-. The Job plot indicates a 2:1 stoichiometry for cyanide−probe **5** interaction. Therefore, the two-step absorption spectral isotherms are ascribed to a double deprotonation process, which is different from the single proton-transfer process observed in probe **2**. The ability to deprotonate the second sulfonamide N−H proton indicates a higher acidity of sulfonamide N−H protons in probe **5** compared to those in probe **2**. The equilibrium constants of the probe **5**−anion interactions are obtained from fitting of the spectral traces and collected in Table 3. The results from Table 3 clearly demonstrated that the sensitivity of both probes **4** and **5** has been significantly raised compared to probes **1** and **2**.

The 2:1 stoichiometry for anion−probe **5** interactions together with a two-step process upon the addition of anions implies that only one sulfonamide ligand is in action with the incoming anions. It seems to be counterintuitive, with three identical sulfonamide N−H interacting sites in probe **5** available for anion binding, which is expected to have an at least 3:1 (anion−probe) binding stoichiometry. Recently, Peng and co-workers reported that the sulfonamide N−H of a receptor 2-[2′-(tosylamino)phenyl]benzoxazole undergoes solvent-induced deprotonation in a DMSO solution.[7a] A similar deprotonation of the 2-[2′-(tosylamino)phenyl]benzimidazole molecule has also been observed in a DMSO solution.[25] We speculate that the coordination of a Ru^{II} metal center to ligand **2** greatly facilitates the ability of N−H proton dissociation in a polar DMSO solution. Therefore, probe **5**

(23) (a) Ion, L.; Morales, D.; Nieto, S.; Pérez, J.; Riera, L.; Miguel, D.; Kowenick, R. A.; McPartlin, M. *Inorg. Chem.* **2007**, *46*, 2846−2853. (b) Peris, E.; Mata, J. A.; Moliner, V. *J. Chem. Soc., Dalton Trans.* **1999**, 3893−3898.

(24) Crabtree, R. H. *The Organometallic Chemistry of the Transition Metals*, 3rd ed.; Wiley: New York, 2001.

(25) Fahrni, C. J.; Henary, M. M.; Van Derveer, D. G. *J. Phys. Chem. A* **2002**, *106*, 7655−7663.

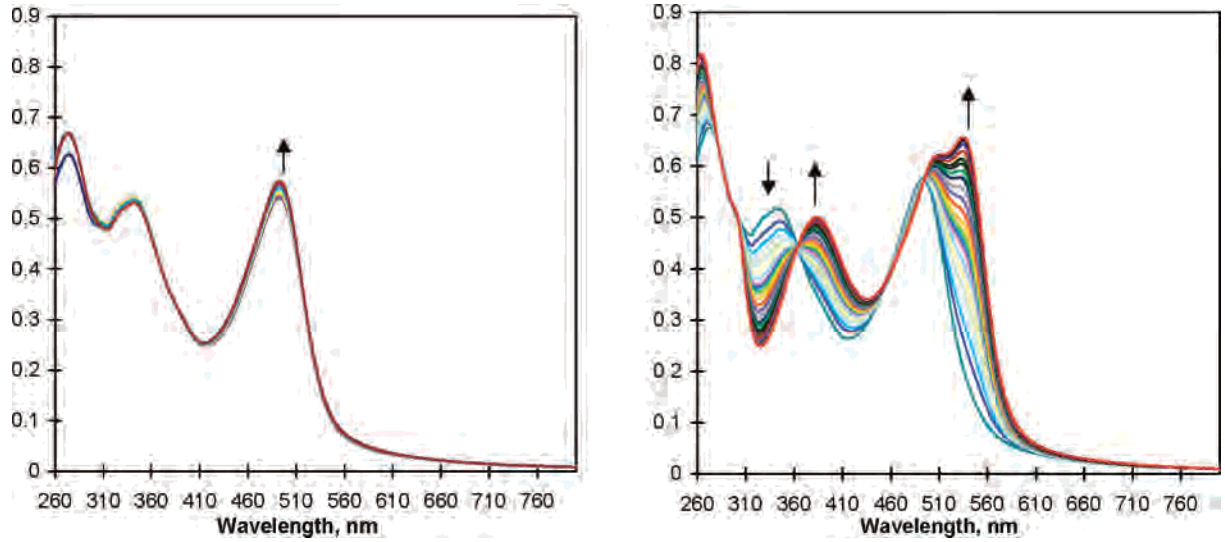

Figure 10. Electronic absorption spectral traces of probe **5** (6.1×10^{-6} M) in DMSO upon the addition of *n*-Bu_4NF. $[F^-] = (0-5.6) \times 10^{-6}$ M (left); $[F^-] = 8.5 \times 10^{-6}-1.7 \times 10^{-3}$ M (right).

becomes a neutral molecule with two N−H protons dissociated at two different ligands that renders only one intact sulfonamide N−H left available for anion interaction.

Conclusion

In conclusion, a series of anion probes featuring sulfonamide interacting sites incorporating to highly chromophoric extended quinoxaline moieties have been prepared and characterized, and their photophysical properties were studied. Their interactions with various anions were also explored by UV−visible, luminescence, and ^{1}H NMR spectroscopy. By variation of the acidity and hydrogen-bonding donor ability of the sulfonamide N−H protons, the sensitivity and selectivity of these probe molecules to anions can be tuned in a simple Brønsted acid−base relationship. The results from ^{1}H NMR spectroscopic experiments provide further evidence for identifying the anion−probe interaction process. The general order of sensitivity is the following: $CN^- > F^- > OAc^- > H_2PO_4^- >> Cl^- > Br^- \approx HSO_4^- \approx NO_3^- \approx ClO_4^-$. The degrees of probe−anion interactions can be easily visualized via naked-eye colorimetric or luminescent responses. In particular, the selectivity for different anions is greatly enhanced upon coordination of organic probes to transition metals. We believe similar quinoxalinesulfonamide receptor−chromophore conjugates can be exploited in the design of efficient sensing molecules for various anionic analytes.

Experimental Section

Materials and General Procedures. *N*,*N*′-(4,5-Diamino-1,2-phenylene)bis(4-methylbenzenesulfonamide) and 1,10-phenanthroline-5,6-dione were synthesized according to a published method.[26,27] All other chemical reagents were commercially available and were used without further purification unless otherwise noted. The anions were used as the tetrabutylammonium salts. NMR spectra were recorded on a Brüker AMX400 (400.168 MHz for ^{1}H NMR and 100.622 MHz for ^{13}C NMR). ^{1}H and ^{13}C NMR chemical shifts are reported in ppm downfield from tetramethylsilane (TMS; δ scale) with the solvent resonances as internal standards. Absorption spectra were obtained using either a Perkin-Elmer Lambda 900 UV−visible−NIR spectrophotometer or a Varian Cary 300 UV−visible spectrophotometer. Emission spectra were recorded in an air-equilibrated CH_3CN or DMSO solution at 298 K with a Fluorolog III photoluminescence spectrometer. Luminescence quantum yields were calculated relative to 9,10-diphenylanthracene in a cyclohexane solution ($\Phi_{em} = 0.90$) or $Ru(bpy)_3Cl_2$ in an air-equilibrated aqueous solution ($\Phi_{em} = 0.028$). Corrected emission spectra were used for the quantum yield measurements. Luminescence quantum yields were taken as the average of three separate determinations and were reproducible to within 10%. Fluorescence lifetimes were measured on an Edinburgh Instruments Mini-t single-photon-counting lifetime spectrometer. The samples were excited at 375 nm from a diode laser with a 80 ps pulse width. Nonlinear least-squares fitting of the decay curves were performed with the Levenburg−Marquardt algorithm and implemented by the Edinburgh Instruments T900 software.

Alternately, luminescence lifetimes were determined on an Edinburgh FL920 time-correlated pulsed single-photon-counting instrument. Samples were degassed via a freeze−thaw−pump cycle at least five times prior to measurements. Samples were excited at 337 nm from a nitrogen-pulsed flashlamp with 1 ns fwhm pulse duration transmitted through a Czerny−Turner design monochromator. Emission was detected at 90° via a second Czerny−Turner design monochromator onto a thermoelectrically cooled red-sensitive photomultiplier tube. The resulting photon counts were stored on a microprocessor-based multichannel analyzer. The instrument response function was profiled using a scatter solution and subsequently deconvoluted from the emission data to yield an undisturbed decay. Nonlinear least-squares fittings of the decay curves were performed with the Levenburg−Marquardt algorithm and implemented by the Edinburgh Instruments F900 software.

Single crystals of **1**, **2**, and **4** were mounted on a glass fiber using oil. All measurements were made on a Brück X8 Apex CCD area detector equipped with graphite-monochromated Mo Kα

(26) Arnold, F. E. *J. Polym. Sci., Polym. Chem. Ed.* **1970**, *8*, 2079−2089.
(27) Dyer, J.; Grills, D. C.; Matousek, P.; Parker, A. W.; Towrie, M.; Weinstein, J. A.; George, M. W. *Chem. Commun.* **2002**, 872−873.

radiation. The structures were solved by direct methods[28a] and refined by a full-matrix least-squares technique based on F^2 using the *SHELXL97* program.[28b] The non-hydrogen atoms were refined anisotropically. Hydrogen atoms were included in idealized positions but not refined. All calculations were performed using the Brüker *SHELXTL* crystallographic software package.[29]

Spectrophotometric titrations were performed using a 2.5 mL probe solution in either CH_3CN or DMSO titrated with a sample of the anions prepared with the same probe solution. Absorption and emission spectra were recorded following each addition of anion.

The equilibrium constants, *K*, were determined by fitting the whole series of spectra at 1 nm intervals using the software *SPECFIT 3.0* from Spectrum Software Associates, which employs a global system with expanded factor analysis and Marquardt least-squares minimization to obtain globally optimized parameters.[30]

Synthesis. Probe 1. A mixture of **6** (750 mg, 1.7 mmol) and **7** (360 mg, 1.7 mmol) in acetic acid (100 mL) was refluxed for 16 h. The volatile mixture was concentrated on a rotary evaporator to ~20 mL, and excess water was added to yield precipitation. The white precipitate was collected on a frit, washed with water and MeOH, and dried in vacuo to afford white powder of **1** (1.0 g, 95%). ^{1}H NMR (400 MHz, DMSO-d_6): δ 10.07 (bs, 2H), 8.23 (d, J = 4.8 Hz, 2H), 7.92−7.86 (m, 4H), 7.74−7.68 (m, 6H), 7.36 (d, J = 8.0 Hz, 4H), 7.32 (t, J = 5.8 Hz, 2H), 2.33 (s, 6H). ^{13}C NMR (75 MHz, acetone-d_6): δ 158.4, 154.0, 148.9, 145.5, 139.6, 137.5, 136.7, 134.6, 130.8, 128.5, 124.8, 124.0, 123.0, 21.5. HRFABMS: *m*/*z* 623.1537 (calcd *m*/*z* 623.1535 for M + H$^+$). Elem anal. Calcd for $C_{32}H_{26}N_6O_4S_2$: C, 61.72; H, 4.21; N, 13.50. Found: C, 61.49; H, 4.48; N, 13.33.

Probe 2. A mixture of **6** (1.0 g, 2.2 mmol) and **8** (470 mg, 2.2 mmol) in MeOH (100 mL) was refluxed for 16 h. Compound **2** precipitated as a microcrystalline solid, which was collected and washed with MeOH and dried in vacuo to afford a yellowish powder of **2** (1.2 g, 91%). ^{1}H NMR (400 MHz, DMSO-d_6): δ 9.50 (d, J = 8.0 Hz, 2H), 9.17 (d, J = 4.0 Hz, 2H), 7.97−7.94 (m, 2H), 7.86 (s, 2H), 7.78 (d, J = 8.4 Hz, 4H), 7.36 (d, J = 8.0 Hz, 4H), 2.32 (s, 6H). A ^{13}C NMR spectrum was not taken due to the very low solubility. HREIMS: *m*/*z* 620.1286 (calcd *m*/*z* 620.1300 for M$^+$). Elem anal. Calcd for $C_{32}H_{24}N_6O_4S_2$: C, 61.92; H, 3.90; N, 13.54. Found: C, 61.76; H, 3.98; N, 13.41.

Probe 3. Essentially the same procedure as that for the preparation of **2** was taken for synthesis of probe **3**. Recrystallization from hot THF afforded a yellowish powder of **3** in 92% yield. ^{1}H NMR (400 MHz, DMSO-d_6): δ 10.10 (bs, 2H), 9.13 (d, J = 8.0 Hz, 2H), 8.74 (d, J = 8.0 Hz, 2H), 7.88 (s, 2H), 7.84 (t, J = 7.6 Hz, 2H), 7.79−7.74 (m, 6H), 7.39 (d, J = 8.0 Hz, 4H), 2.33 (s, 6H). ^{13}C NMR (75 MHz, DMSO-d_6): δ 141.9, 139.9, 139.3, 139.0, 138.0, 130.4, 130.0, 129.4, 129.2, 127.8, 126.5, 124.8, 123.3, 109.2, 30.7. HREIMS: *m*/*z* 618.1385 (calcd *m*/*z* 618.1395 for M$^+$). Elem anal. Calcd for $C_{34}H_{26}N_4O_4S_2$: C, 66.00; H, 4.24; N, 9.06. Found: C, 65.95; H, 4.15; N, 9.11.

Probe 4. A mixture of $BrRe(CO)_5$ (200 mg, 0.50 mmol) and ligand **1** (150 mg, 0.24 mmol) in 50 mL of THF was refluxed under a nitrogen atmosphere for 12 h. The resulting orange precipitate was collected on a frit, washed with cold THF and diethyl ether, and dried under vacuum to afford an orange-red powder of **4** (310 mg, 97%). ^{1}H NMR (400 MHz, CD_3CN): δ 9.15 (d, J = 5.5 Hz, 2H), 8.46 (s, 2H), 8.31 (d, J = 8.2 Hz, 2H), 7.94 (t, J = 6.7 Hz, 2H), 7.75 (d, J = 8.3 Hz, 4H), 7.59 (t, J = 6.3 Hz, 2H), 7.25 (d, J = 8.2 Hz, 4H), 2.30 (s, 6H). HRFABMS: *m*/*z* 1321.8634 (calcd *m*/*z* 1321.8634 for M$^+$). Elem anal. Calcd for $C_{38}H_{26}Br_2N_6O_{10}Re_2S_2$: C, 34.50; H, 1.98; N, 6.35. Found: C, 34.42; H, 2.06; N, 6.31.

Probe 5. A mixture of $RuCl_3 \cdot 3H_2O$ (27 mg, 0.10 mmol) and ligand **2** (200 mg, 0.32 mmol) in 35 mL of ethylene glycol was heated at 150 °C under a nitrogen atmosphere for 3 h. After the solution was cooled to room temperature, the saturated aqueous NH_4PF_6 (10 mL) solution was added in one portion. The mixture was stirred at room temperature for 2 h. The resulting precipitate was collected on a frit, washed with water and diethyl ether, and dried under vacuum. Repeated recrystallization from hot CH_3CN afforded 100 mg of a reddish-brown solid in 14% yield. ^{1}H NMR (400 MHz, DMSO-d_6): δ 9.45 (d, J = 8.2 Hz, 2H), 8.13 (d, J = 8.8 Hz, 2H), 7.75−7.70 (m, 8H), 7.26 (d, J = 7.7 Hz, 4H), 2.27 (s, 6H). HRFABMS: *m*/*z* 1961.2889 (calcd *m*/*z* 1961.2867 for [M − 2PF$_6$ − H$^+$]$^+$). Elem anal. Calcd for $C_{96}H_{72}F_{12}N_{18}O_{12}P_2RuS_6 \cdot H_2O$: C, 50.77; H, 3.28; N, 11.10. Found: C, 50.65; H, 3.31; N, 10.93.

Acknowledgment. We are grateful to the National Science Council of Taiwan (Grants 94-2113-M-001-014 and 95-2113-M-001-033-MY2) and Academia Sinica for support of this research.

Supporting Information Available: X-ray crystallographic details in CIF format and anion titration spectra. This material is available free of charge via the Internet at http://pubs.acs.org.

IC701300A

(28) (a) Sheldrick, G. M. *SHELXS97, Program for Crystal Structure Solution*; University of Göttingen: Göttingen, Germany, 1997. (b) Sheldrick, G. M. *SHELXL97, Program for Crystal Structure Solution*; University of Göttingen: Göttingen, Germany, 1997.

(29) *Shelxtl for WindowsNT: Crystal Structure Analysis Package*, Brüker: Madison, WI, 1997.

(30) (a) *SPECFIT*, version 3.0; Spectra Software Associates: Claix, France, 2005. (b) Gampp, H.; Maeder, M.; Meyer, C. J.; Zuberbühler, A. D. *Talanta* **1985**, *32*, 95−101. (c) Gampp, H.; Maeder, M.; Meyer, C. J.; Zuberbühler, A. D. *Talanta* **1986**, *33*, 943−951.